Laboratory gouge friction: Seismic-like slip weakening and secondary rate- and state-effects

Guillaume Chambon, Jean Schmittbuhl, Alain Corfdir

Laboratory gouge friction: Seismic-like slip weakening and secondary rate- and state-effects

Guillaume Chambon and Jean Schmittbuhl
Laboratoire de Géologie, École Normale Supérieure, Paris, France

Alain Corfdir
CERMES, ENPC/LCPC, Champs sur Marne, France

Received 27 November 2001; revised 6 February 2002; accepted 4 March 2002; published 16 May 2002.

[1] We investigate experimentally the frictional response of a thick sample of simulated fault gouge submitted to very high shear displacements (up to 40 m) in an annular simple shear apparatus (ACSA). The frictional strength of our granular material exhibits velocity-weakening consistent with classical rate- and state-dependent friction laws. The length scale involved in the latter phenomenon is d_c = 100 μm. However, the evolution of friction is largely dominated by a significant slip-weakening active over decimetric distances (L = 0.5 m). Interestingly, these decimetric frictional length scales are quantitatively compatible with those estimated for natural faults. During shearing, a thin and highly-sheared layer emerges from the thick and slowly-deforming bulk of the sample. Because of the intermittent and non-local coupling observed between these two zones, we relate the large frictional length scales in our data to the slow structuring of the thick interface. *INDEX TERMS:* 7209 Seismology: Earthquake dynamics and mechanics; 8010 Structural Geology: Fractures and faults; 8123 Tectonophysics: Dynamics, seismotectonics; 8025 Structural Geology: Mesoscopic fabrics; 8159 Tectonophysics: Evolution of the Earth: Rheology—crust and lithosphere

1. Introduction

[2] Understanding fault friction represents a key element toward a comprehensive description of the seismic cycle. Two decades of experimental studies on the mechanical behavior of rock-rock and rock-gouge interfaces resulted in the formulation of two classes of friction laws [*Dieterich*, 1979; *Ruina*, 1983; *Ohnaka and feng Shen*, 1999; *Marone*, 1998]: the rate- and state-dependent friction (RSF) laws, and the slip-dependent laws. RSF laws, in particular, successfully account for many properties of the natural seismicity [*Rice*, 1993; *Dieterich*, 1994]. However, quantitative earthquake modeling usually requires friction weakening distances of about 10^{-2}–1 m [*Ide and Takeo*, 1997; *Bouchon et al.*, 1998; *Guatteri and Spudich*, 2000], whereas typical length scales involved in laboratory effects are in the range 10^{-6}–10^{-4} m. To face this difficulty, a classical approach [*Scholz*, 1988; *Marone and Kilgore*, 1993; *Ohnaka and feng Shen*, 1999] consists in applying scaling procedures to the laboratory-derived constitutive parameters (particularly the characteristic lengths). Here, we look for alternative frictional mechanisms which could involve length scales directly compatible with seismological estimations. In particular, gouge samples in experimental fault studies are rarely wider than 10–20 grains (i.e., a few mm) [*Marone et al.*, 1990; *Beeler et al.*, 1996]. Along real faults, however, the gouge layers can reach thicknesses of several meters after repeated slipping events [*Scholz*, 1997]. The aim of this letter is to explore the frictional behavior of thicker samples of simulated gouge submitted to high shear strains.

0094-8276/02/2001GL014467

2. Experimental Setup

[3] We performed gouge shearing experiments in a pseudo-Couette apparatus sketched in Figure 1 [*Lerat*, 1996]. The ring-shaped sample of dense quartz sand is about 100 grain-thick, and the circumference of the sand-steel interface is 600 grains. (The mean grain diameter is 1 mm.) With this setup, plurimetric and rigorously uniform shear displacement fields can be imposed to sample inner boundary. A roughness comparable to grain size, machined on the surface of the rotating cylinder, insures transmission of strain inside the granular material. During shearing, the sample is submitted to a constant radial confining stress σ (non-rigid outer boundary). In what follows, we regard the shear flow in our experiments as essentially 2D, thus neglecting influences of the top and bottom plates embedding the gouge. In particular, we have indications that the mean normal stress on sample inner boundary consistently stabilizes at a value about twice the confining pressure σ after a few millimeters of slip. This observation rules out a Janssen-like [*Duran*, 2000] screening of the radial confining stress by friction along the top and bottom walls.

3. Velocity-Weakening

[4] We first examine the frictional response of our simulated gouge to prescribed changes in shear velocity (Figure 2). As in most other studies, the range of accessible velocities of our apparatus (10^{-6}–10^{-4} m s^{-1}) is medianly situated between tectonic and seismic slip rates (of the order of 10^{-11}–10^{-10} and 10^{-1}–1 m s^{-1}, respectively [*Scholz*, 1997]). An increase of the shear velocity by a factor of 60 is found to trigger a decrease of about 10% in the normalized shear stress on sample inner boundary, τ/σ (equivalent to the shear stress τ since σ is held constant during our runs) (Figure 2). The transient regime leading to the new steady-state level $(\tau/\sigma)_{ss}$ consists of one major drop, which appears more rapid than the velocity evolution, followed by a few damped oscillations (Figure 2b). Several realizations at a given shear velocity yield a significant variability in $(\tau/\sigma)_{ss}$ (Figure 2c). Nevertheless, a logarithmic trend emerges between the steady-state effective friction and velocity, at least for small shear displacements δ (Figure 2c). All these features are consistent with classical RSF laws, and we compute a value of the RSF constitutive parameter $B - A$ of 1.4×10^{-2}, fully compatible with previous studies [*Beeler et al.*, 1996]. However, when the cumulative shear displacement imposed to the sample increases, fluctuations become larger and correlation between $(\tau/\sigma)_{ss}$ and shear velocity progressively vanishes, up to a complete loss of RSF validity for $\delta > 3$–4 m (Figure 2c). From

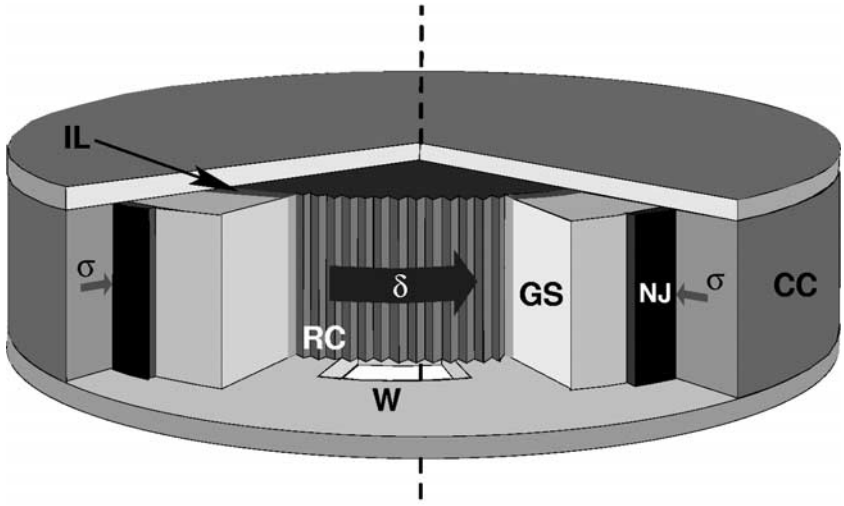

Figure 1. Sketch of the annular simple shear apparatus. A rough steel cylinder (**RC**) is rotated at an imposed velocity $c = d\delta/dt$ inside a ring-shaped granular sample (**GS**) (velocity range: 1.7–100 μm s^{-1}). Cylinder radius is 100 mm and sample radial section is 100 mm × 100 mm. Fault gouge is simulated by a quarry sand exclusively composed of angular quartz grains and sieved between 0.80 and 1.25 mm to achieve a grain distribution median of 1 mm. Initial porosity of the samples is about 40%. Measurements of the torque exerted on the cylinder by the driving system give access to the shear stress τ on sample inner boundary. The outer boundary of the gouge is encased in a neoprene jacket (**NJ**) and undergoes radial confinement at constant pressure σ imposed by a water cell (**CC**). While small radial deformations are allowed by the jacket, vertical displacements are precluded by the two rigid plates embedding the sample. A glass window (**W**) pierced in the lower part of the bottom plate enables direct visual observation of about 80% of sample width, including the interfacial layer (**IL**).

Figure 2b we can also infer (visually or with a simple spring-slider model taking into account RSF and finite duration velocity changes) that the length scale involved in RSF phenomena in our data is about d_c = 100 μm. This value approaches the resolution limit of our rotation encoder (70 μm), but, though a little large, is compatible with previous results [*Marone and Kilgore*, 1993; *Beeler et al.*, 1996].

4. Slip-Weakening

[5] Though noticeable, shear stress alterations of a few percents by velocity-weakening constitute a second-order effect in our data: they are superimposed on a major slip-weakening trend (Figure 3a). When shearing is initiated on a fresh gouge sample, τ increases during the first 10 mm of displacement δ and reaches a peak value (Figure 3a). Subsequent slip then induces a marked weakening of the shear stress which drops by 50–70% down to a residual plateau value of about 0.3 σ (for a constant shear velocity of 8 × 10^{-5} μm s^{-1}) (Figure 3a). We checked that this weakening effectively is slip-, and not time-, induced: disregarding second-order ageing effects, τ is unaffected by hold periods at zero velocity imposed to the sample. The characteristic distance involved in shear stress decrease is remarkably large compared to the RSF length scale, of the order of L = 0.5 m (Figure 3a). Interestingly, slip-weakening does not appear as an irreversible process for a given gouge sample. In particular, changes of the rotation sense are found to trigger significant restrengthening of the shear stress (Figure 3a). To a lesser extent, a prescribed drop of τ also induces restrengthening when shear is resumed. Such restrengthening probably results from particle rearrangements and re-consolidation inside the granular sample [*Nakatani*, 1998]. Whenever τ passes through a peak (more than 50 experiments were performed), it then consistently undergoes the same extraordinary slip-weakening process over decimetric distances (Figure 3a). This weakening thus constitutes an intrin-

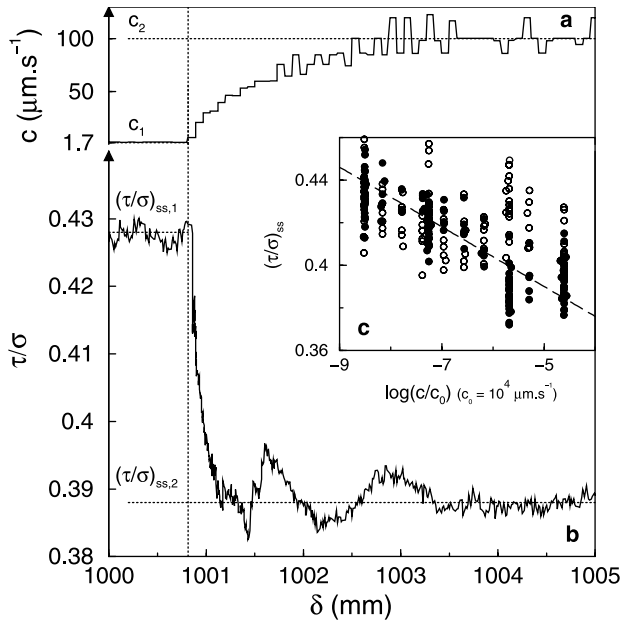

Figure 2. Velocity dependence of effective friction. (a) Evolution of the shear velocity c, as a function of displacement δ, resulting from a prescribed velocity increase from c_1 = 1.7 μm s^{-1} to c_2 = 100 μm s^{-1}. (b) Evolution of the normalized shear stress τ/σ in response to this velocity increase. The values $(\tau/\sigma)_{ss,\,1}$ and $(\tau/\sigma)_{ss,2}$ characterize the steady-state frictional regimes reached for $c = c_1$ and $c = c_2$, respectively. (c) Plot of the steady-state normalized shear stress $(\tau/\sigma)_{ss}$ versus normalized shear velocity c/c_0 (semi-logarithmic scale). Shear phases corresponding to 0.6 < δ < 3 m and to 3.6 < δ < 6 m are separated on the plot (• and ○, respectively). The dashed straight line (slope: $A - B = -1.4 \times 10^{-2}$) is the best fit of the small-δ data.

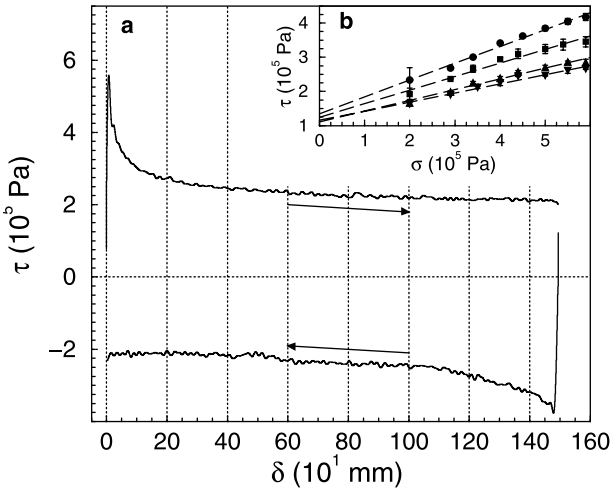

Figure 3. Slip dependence of effective friction. (a) Plot of the shear stress τ versus displacement δ for two slip phases in opposite senses indicated by arrows ($\sigma = 5 \times 10^5$ Pa, $c = 8 \times 10^{-5}$ μm s^{-1}). The sample is fresh at the onset of the $\tau > 0$ phase. (b) Results of various shear runs conducted at different confining stresses: evolution of the shear stress τ as a function of σ for fixed values of the partial displacement δ. The four data sets (●, ■, ▲, and ▼) correspond to δ values of 20, 100, 300, and 500 mm, respectively. Error bars represent the difference between two realizations of each experiment. The dashed lines are the linear best fits of the data sets.

sic attribute of our simulated fault, and should not be merely regarded as the erasure of some initial properties of the sample that would have been inherited from its preparation [*Bystricky et al.*, 2000].

5. Comparison With Faults

[6] We evidenced two independent processes affecting gouge strength in our experiments. RSF-like phenomena result in a second-order velocity-weakening, probably related to microscopic mechanisms active at grain-grain contacts [*Dieterich*, 1979; *Scholz*, 1988]. On the contrary, the dominant effect is a slip-weakening whose amplitude and characteristic distance cannot be accounted for in the classical RSF framework. An outstanding result is the good qualitative and quantitative agreement between slip-weakening in our experiments and the typical friction laws derived from earthquake modeling, particularly with respect to the characteristic distances. Fault strength is generally expressed in terms of an intrinsic coefficient of friction. We performed shear runs at various confining stresses (Figure 3b). They indicate that, at any displacement δ, the shear stress τ on sample inner boundary depends linearly on the external stress σ. Accordingly, an effective friction coefficient μ_f can also be defined for our simulated fault: $\tau = \mu_f(\delta) \times \sigma + C_f$, where the effective cohesion C_f is roughly independent of δ. The effective friction coefficient μ_f depends generally on the whole loading history, but this dependence reduces, for shear paths at constant σ, to a simple slip-dependence, namely, a significant, seismic-like slip-weakening. Just as for faults, introducing this effective friction constitutes an upscaling procedure in which the whole gouge layer is regarded as a "thick interface" and its bulk mechanics reduced to an interfacial law.

6. Gouge Microstructure

[7] Analysis of the post-weakening structure developed inside the gouge for $\delta > 1-2$ m reveals complex features (Figure 4). Numerous fine particles have appeared in a narrow interfacial layer near the inner cylinder (Figure 4a). The width of this interfacial layer corresponds to 6–7 initial grains. However, rapid and continuous shear deformation takes place only in an inner portion of the comminuted interfacial layer, which has presumably reached its "critical state" (in the soil mechanics sense) (Figure 4b). The whole rest of the gouge also deforms, but in a slow and discontinuous manner dominated by burst-like events during which a certain number of grains reorganize (or break, for those particles inside the interfacial layer but not in continuous motion). These bursts appear emitted by the continuously moving layer and can affect particle clusters of all sizes (up to 40–50 grains at least) (Figure 4b), the smaller being the more frequent. Hence, the zone of active deformation inside the gouge is in fact highly changing with time and, at a given moment, appears as a

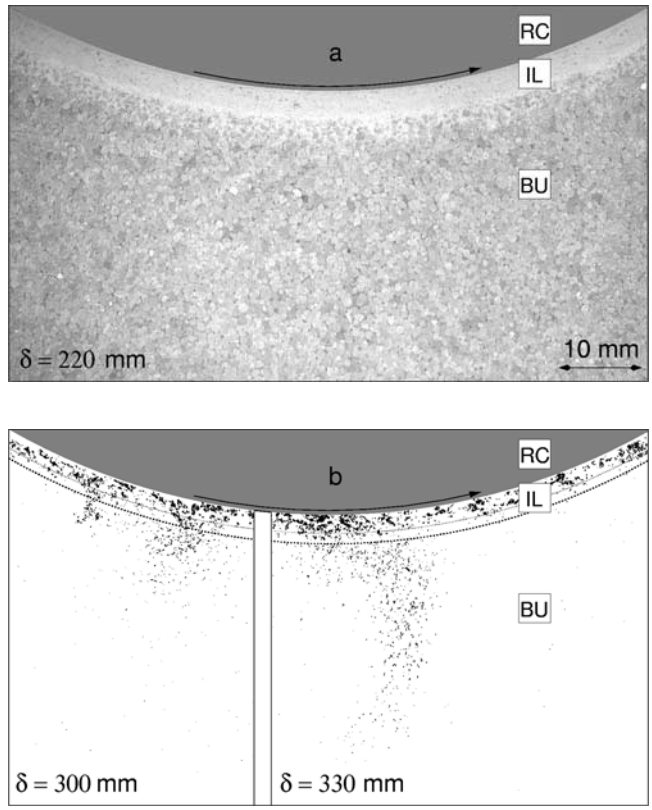

Figure 4. Gouge structuring. (a) Photograph of sample bottom surface (through the window, see Figure 1). The shaded area in the upper part of the picture corresponds to the inner cylinder (**RC**), rotating from right to left. Sand grains can easily be identified in the bulk of the sample (**BU**), except in a narrow interfacial layer near the inner cylinder where the material is comminuted (**IL**). For this photo, δ = 2.2 m. (b) Localization of particle displacements inside the gouge for δ = 3 m (left part of the picture) and δ = 3.3 m (right part). The not-displayed portions of both images consist of white areas except near the inner cylinder. Particle displacements are tracked by computing the pixel to pixel difference between two successive photographs of sample bottom surface, taken with a delay of 10 s (which corresponds to a 0.8 mm rotation of the inner cylinder). Each black spot in the images highlights a zone where grain displacements of at least 10 μm are recorded. The thick dashed line, inferred from panel a, represents the structural boundary delimiting the comminuted interfacial layer (**IL**). The thin dotted line, on the contrary, materializes a mechanical boundary between a region where grains are in continuous motion (inner part of the interfacial layer), and a region submitted to intermittent and inhomogeneous deformation (the whole rest of the sample).

rough layer developing outgrowths over a wide range of length scales.

7. Discussion

[8] We checked that the large slip-weakening distance in our data does not directly scale with grain size or system dimensions. Specifically, the shear stress evolution in Figure 3a remains completely unchanged when using 0.6 mm instead of 1 mm sand. To us, slip-weakening over decimetric distances should be related to gouge structuring. We believe that it arises from the progressive formation and evolution inside the sample of two interacting zones exhibiting very different deformation modes, as described in the previous paragraph. Working with a thick gouge sample (i.e., significantly wider than 6–7 initial grains) appears as a necessary condition for complexity to develop inside the material, and thus for the emergence of large frictional characteristic distances. In other studies which limit consideration to thin gouge samples sandwiched between two solid walls [*Marone et al.*, 1990; *Beeler et al.*, 1996], these distances are probably inhibited (except maybe at high slip rates [*Goldsby and Tullis*, 1999]). Clearly, these hypotheses need to be confirmed by further experiments and numerical modeling, to assess in particular the precise influence of sample thickness on the mechanical response.

[9] Even if their similarity with seismological friction laws is remarkable, extrapolation of our results to natural faults still remains a difficult issue (as for all the other experimental fault studies). In our case, objections arise in particular from the cylindrical geometry of the shear interface, which is known to promote localization of deformation compared to plane shear setups. Also, hoop stresses could in principle develop or fluctuate in our cylindrical samples and induce artifactual changes in apparent friction. However, the continual remobilization of regions of all sizes inside the gouge, the clear existence of an effective friction coefficient, and the smallness of force correlation lengths in non-cohesive granular materials [*Radjai et al.*, 1999], suggest that hoop stresses probably play a negligible role in our experiments. In spite of these open questions, interesting geophysical perspectives already arise from our results. Indeed, the combined observation of a slip-weakening and a restrengthening mechanisms may offer a new framework, independent of classical RSF phenomena, for interpreting and modeling earthquake recurrence on gouge-filled faults. This novel interpretation would present the advantage of directly accounting for decimetric to metric friction weakening distances.

[10] **Acknowledgments.** Experiments were conducted at the CERMES, ENPC/LCPC, Marne-la-Vallée, France. We thank J. P. Vilotte, J. Sulem, and P. Lerat for fruitful discussions. We also acknowledge J. Dieterich, J. Rice, and T. Tullis for extended and helpful comments.

References

Beeler, N. M., T. E. Tullis, M. L. Blanpied, and J. D. Weeks, Frictional behavior of large displacement experimental faults, *J. Geophys. Res.*, *101*, 8697–8715, 1996.

Bouchon, M., H. Sekiguchi, K. Irikura, and T. Iwata, Some characteristics of the stress field of the 1995 Hyogo-ken Nanbu (Kobe) earthquake, *J. Geophys. Res.*, *103*, 24,271– 24,282, 1998.

Bystricky, M., K. Kunze, L. Burlini, and J. Burg, High shear strain of olivine aggregates: Rheological and seismic consequences, *Science*, *290*, 1564–1567, 2000.

Dieterich, J., A constitutive law for rate of earthquake production and its application to earthquake clustering, *J. Geophys. Res.*, *99*, 2601–2618, 1994.

Dieterich, J. H., Modeling of rock friction, 1, Experimental results and constitutive equations, *J. Geophys. Res.*, *84*, 2161–2168, 1979.

Duran, J., *Sands, Powders, and Grains: An Introduction to the Physics of Granular Materials*, Springer, Berlin, 2000.

Goldsby, D. L., and T. E. Tullis, Extraordinary frictional weakening at rapid subseismic slip rates, *EOS Trans. AGU*, *80*(46), Fall. Meet. Suppl, 1999.

Guatteri, M., and P. Spudich, What can strong-motion data tell us about slip-weakening fault-friction laws?, *Bull. Seismol. Soc. Am.*, *90*, 98–116, 2000.

Ide, S., and M. Takeo, Determination of constitutive relations of fault slip based on seismic wave analysis, *J. Geophys. Res.*, *102*, 27,379–27,391, 1997.

Lerat, P., Etude de l'interface sol-structure dans les milieux granulaires à l'aide d'un nouvel appareil de cisaillement annulaire, Thèse de doctorat, École Nationale des Ponts et Chaussées, 1996.

Marone, C., Laboratory–derived friction laws and their application to seismic faulting, *Annu. Rev. Earth Planet. Sci.*, *26*, 643–696, 1998.

Marone, C., and B. Kilgore, Scaling of the critical slip distance for seismic faulting with shear strain in fault zones, *Nature*, *362*, 618–621, 1993.

Marone, C., C. B. Raleigh, and C. H. Scholz, Frictional behavior and constitutive modeling of simulated fault gouge, *J. Geophys. Res.*, *95*, 7007–7025, 1990.

Nakatani, M., A new mechanism of slip weakening and strength recovery of friction associated with the mechanical consolidation of gouge, *J. Geophys. Res.*, *103*, 27,239–27,256, 1998.

Ohnaka, M., and L. F. Shen, Scaling of the shear rupture process from nucleation to dynamic propagation: Implications of geometric irregularity on the rupturing surfaces, *J. Geophys. Res.*, *104*, 817–844, 1999.

Radjai, F., S. Roux, and J.-J. Moreau, Contact forces in a granular packing, *Chaos*, *9*, 544–550, 1999.

Rice, J. R., Spatio-temporal complexity of slip on a fault, *J. Geophys. Res.*, *98*, 9885–9907, 1993.

Ruina, A., Slip instability and state variable friction laws, *J. Geophys. Res.*, *88*, 10,359–10,370, 1983.

Scholz, C. H., The critical slip distance for seismic faulting, *Nature*, *336*, 761–763, 1988.

Scholz, C. H., *The Mechanics of Earthquakes and Faulting*, Cambridge Univ. Press, Cambridge, 1997.

G. Chambon and J. Schmittbuhl, Laboratoire de Géologie, UMR CNRS 8538, École Normale Supérieure, 24, rue Lhomond, F-75231 Paris Cédex 05, France. (chambon@ens.fr; Jean.Schmittbuhl@ens.fr)

Alain Corfdir, CERMES, ENPC/LCPC, 6 et 8 avenue Blaise Pascal, 77455 Champs sur Marne, France. (corfdir@cermes.enpc.fr)